Structural and Spectral Properties of 4-Bromo-1-naphthyl Chalcones: A Quantum Chemical Study

4 AUTHORS, INCLUDING:

Nithya Raja
Bharathiar University
6 PUBLICATIONS 36 CITATIONS

SEE PROFILE

Santhanamoorthi Nachimuthu
National Taiwan University of Science and Te…
32 PUBLICATIONS 191 CITATIONS

SEE PROFILE

K. Senthilkumar
Bharathiar University
77 PUBLICATIONS 1,444 CITATIONS

SEE PROFILE

Structural and Spectral Properties of 4-Bromo-1-naphthyl Chalcones: A Quantum Chemical Study

R. Nithya, N. Santhanamoorthi, P. Kolandaivel, and K. Senthilkumar*

Department of Physics, Bharathiar University, Coimbatore, India 641 046

Ⓢ *Supporting Information*

ABSTRACT: The structural and optical properties of 4-bromo-1-naphthyl chalcones (BNC) have been studied by using quantum chemical methods. The density functional theory (DFT) and the singly excited configuration interaction (CIS) methods were employed to optimize the ground and excited state geometries of unsubstituted and substituted BNC with different electron withdrawing and donating groups in both gas and solvent phases. Based on the ground and excited state geometries, the absorption and emission spectra of BNC molecules were calculated using the time-dependent density functional theory (TDDFT) method. The solvent phase calculations were performed using the polarizable continuum model (PCM). The geometrical parameters, vibrational frequencies, and relative stability of *cis-* and *trans-*isomers of unsubstituted and substituted BNC molecules have been studied. The results from the TDDFT calculations reveal that the substitution of electron withdrawing and electron donating groups affects the absorption and emission spectra of BNC.

Unsubstituted trans BNC
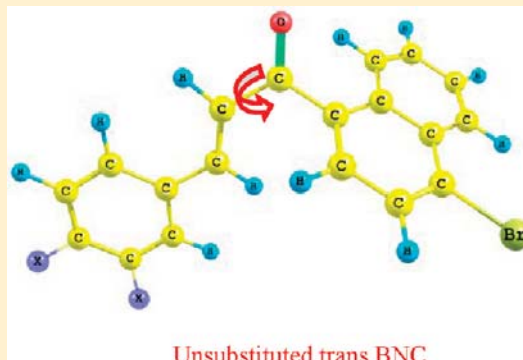
1. INTRODUCTION

Chalcones are organic compounds having interesting optical properties including high excitation coefficients for absorption in the UV region and nonlinear optical responses.[1,2] Chalcones are used as UV-absorption filters, optical sensor materials in the food industry, and in holographic recording technologies.[3,4] In the past two decades, numerous biological applications have also been proposed for these compounds including antiulcer, anticancer, antifungal, anti-HIV, antioxidant activities, and etc.,[5−9] The photophysical properties of substituted chalcones have been studied by many researchers involving mostly asymmetrical donor—acceptor chalcones[10−12] and to a minor extent symmetrical donor—acceptor chalcones. Recently, Thirunarayanan et al.[13] have synthesized the 4-bromo-1-naphthyl chalcones (BNC) by the crossed-aldol condensation of aromatic ketones with benzaldehydes. It has been shown that the BNC exist in two isomers i.e, the s-cis and s-trans forms (see Figure 1). They have analyzed the IR and NMR spectral properties of BNC with various substitutions. It is expected that this type of molecules possess good photoluminescence properties and different substitution of electron withdrawing group (EWG) and electron donating group (EDG) will alter structure, energy, and optical properties. Hence, it is important to study the structure, energy, and optical properties of BNC with different substitutions. In the present study, the electron withdrawing groups CF_3, NO_2, and CN and the electron donating groups $N(CH_3)_2$, OCH_3, and OH are substituted at para and meta positions of BNC.

The results obtained from quantum chemical calculations are used to investigate the relationship between the electronic structure and spectral properties of the unsubstituted, EWG-, and EDG-substituted

BNC. The optical properties of materials involve both occupied and unoccupied states. The time-dependent density functional theory (TDDFT)[14,15] and configuration interaction singles (CIS)[16] are the most popular quantum chemical methods used to calculate the excited state properties of medium-sized molecules. The TDDFT method is a powerful approach to model the electronic transitions and excited state geometries of inorganic and organic molecules.[17−21] The TDDFT method is well suited to study large systems because of its low computational cost compared to wave function based quantum chemical methods.[22,23] However, the accuracy of the TDDFT depends on the so-called adiabatic approximation,[14,15] and approximate ground-state exchange-correlation functional used in the DFT calculations.[24] The TDDFT method has its limitations in the optimization of the excited state geometry and the calculation of long-range excited state charge transfer. This is due to the self-interaction error in the orbital energies and incorrect asymptotic behavior of the standard exchange correlation functional employed.[25,26] It has been shown in earlier studies that the combined CIS and TDDFT methods provide accurate results for excited state properties of organic molecules.[27,28] Previous studies on ground and excited state properties of conjugated polymers and chalcones show that the performance of the TDDFT method with B3LYP and PBE1PBE functionals is good.[27−29] To the best of our knowledge there is no experimental or theoretical studies
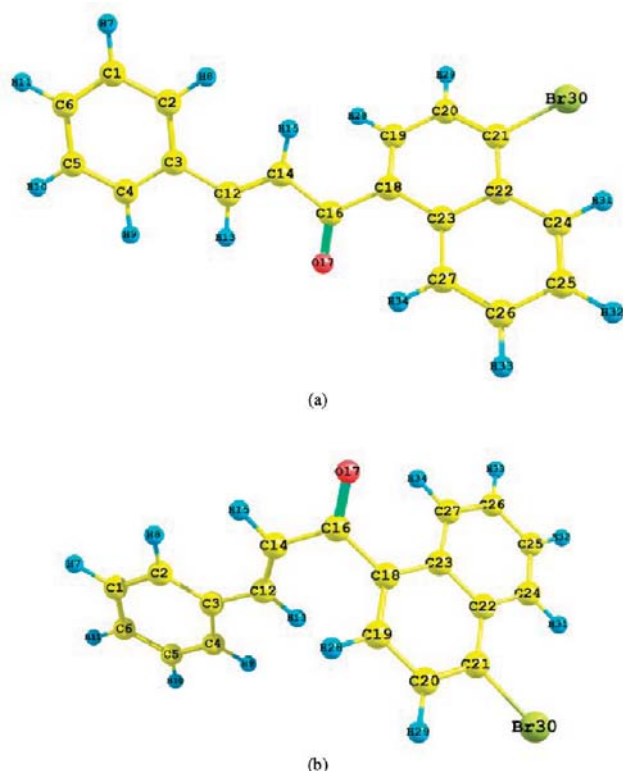
Figure 1. Optimized structures of unsubstituted (a) *cis*- and (b) *trans*-isomers of BNC at B3LYP/6-311G(d,p) level of theory.

Table 1. Relative Energy, $\Delta E = E_{cis} - E_{trans}$ (in kcal/mol) of Unsubstituted and Substituted BNC Calculated at (A) B3LYP/6-311G(d,p), (B) PBE1PBE/6-311G(d,p), (C) MP2/6-311G(d,p), (D) MP2/6-311G(2d,2p)//B3LYP/6-311G(d,p), and (E) B3LYP/6-311G(d,p)[a] Levels of Theory in the Gas Phase and the Ground State Dipole Moment (in Debye) of the *Trans*-Isomer Calculated at the B3LYP/6-311G(d,p) Level of Theory in Gas and Ethanol Medium

	relative energy ΔE (kcal/mol)					dipole moment (Debye)	
BNC molecule	A	B	C	D	E	gas	ethanol
unsubstituted	−1.51	−1.19	0.25	0.06	−1.51	3.60	5.07
CF$_3$	0.19	0.25	0.19	0.25	0.19	2.52	2.49
NO$_2$	0.38	0.38	0.32	0.31	0.38	5.42	6.14
CN	0.19	0.13	0.13	0.13	0.19	5.70	6.63
N(CH$_3$)$_2$	−1.63	−1.32	0.32	0.13	−1.63	6.23	8.96
OCH$_3$	0.44	0.50	0.50	0.50	0.44	4.36	5.50
OH	0.25	0.25	0.32	0.31	0.25	3.06	4.20

[a] MP2/6-311G(d,p) optimized geometry was used as the starting structure.

the self-consistent reaction field (SCRF) calculation has been performed using Tomasi's[39] polarizable continuum model (PCM). In the PCM method, the solute molecule is lying inside a cavity representing a solvent medium defined in terms of structureless material characterized by its dielectric constant, radius, density, and molecular volume. In the present study, the dielectric constant of 24.85 is used to represent the ethanol medium. The quantum chemical calculations were performed using the Gaussian 09 program package.[40]

3. RESULTS AND DISCUSSION

3.1. Molecular Structure, Energy, and Dipole Moment. The geometry of *cis*- and *trans*-isomers of unsubstituted and substituted 4-bromo-1-naphthyl chalcones (BNC) were optimized at B3LYP/6-311G(d,p), PBE1PBE/6-311G(d,p), and MP2/6-311G(d,p) levels of theory. The relative energies calculated for unsubstituted and substituted BNC molecules are summarized in Table 1. The calculated relative energy for unsubstituted molecule at B3LYP/6-311G(d,p) level of theory show that the *cis*-isomer is more stable by 1.51 kcal/mol than the *trans*-isomer. While substituting the different electron withdrawing and donating groups at para and meta positions of BNC, the *trans*-isomer is stabilized more compared to the *cis*-isomer, except for N(CH$_3$)$_2$-substituted BNC, in which the *cis*-isomer is found to be more stable by 1.63 kcal/mol. It has been observed that, at the B3LYP/6-311G(d,p) level of theory, the calculated relative energy is less than 0.50 kcal/mol for all the substitutions except for the N(CH$_3$)$_2$-substituted BNC molecule. It has been noted that the calculated relative energy at the PBE1PBE/6-311G(d,p) level of theory has the same trend as observed in the B3LYP method (see Table 1). Recent DFT studies on chalcone derivatives[29,41] show that the *trans*-isomer is more stable than the *cis*-isomer. The steric effect between the carbonyl group and the naphthyl ring makes the *cis*-isomer slightly less stable.[29] Hence, the geometry of the unsubstituted, EWG- and EDG-substituted *cis*- and *trans*-isomers of BNC were optimized at the MP2/6-311G(d,p) level of theory. The relative energy calculated at the MP2/6-311G(d,p) level of theory for unsubstituted

2. COMPUTATIONAL DETAILS

The ground state geometry of unsubstituted and different electron withdrawing and donating groups substituted BNC has been optimized using DFT methods B3LYP,[30−33] PBE1PBE,[34−37] and second order Møller−Plesset perturbation theory (MP2).[38] The B3LYP functional uses the Becke's three parameter exchange functional (B3)[30] together with the nonlocal correlation function provided by Lee−Yang−Parr (LYP)[31] and the local correlation functional of Vosko−Wilk−Nusair (VWN).[32] The PBE functional of Perdew−Burke−Ernzerhof[34,35] was made into a hybrid functional by Adamo[36] as PBE1PBE, which includes 25% exchange and 75% correlation. The atomic basis set 6-311G(d,p) is used in all the ground state optimizations. The frequency calculations have been performed at the B3LYP/6-311G(d,p) level of theory. The excited state geometry of unsubstituted and substituted BNC molecules has been optimized by using the singly excited configuration interaction (CIS)[16] method with the 6-31+G(d,p) basis set. With the ground and excited state geometries, the absorption and emission spectras were computed by using time-dependent density functional theory (TDDFT)[14,15] methods at B3LYP/6-311G(d,p) and PBE1PBE/6-311G(d,p) levels of theory. To study the solvent polarity effects,

available on absorption and emission spectra of substituted BNC molecules. Hence, in the present investigation, TDDFT and CIS methods are used to investigate the absorption and emission spectra of unsubstituted and substituted BNC. In addition to this, the present theoretical study will provide structural and other basic properties such as conformational stability, vibrational frequencies, and dipole moment of unsubstituted and substituted BNC.

6595

dx.doi.org/10.1021/jp1098393 |*J. Phys. Chem. A* 2011, 115, 6594−6602

and substituted BNC molecules show that the *trans*-isomer is more stable than the *cis*-isomer and the relative energy is less than 0.50 kcal/mol for all the BNC molecules. The results obtained from single point energy calculation performed at MP2/6-311G(2d,2p)//B3LYP/6-311G(d,p) level of theory is in agreement with the results obtained at MP2/6-311G(d,p) level of theory. Further, the BNC molecules were optimized at B3LYP/6-311G(d,p) method with the MP2/6-311G(d,p) optimized geometry as the starting geometry. As given in Table 1, the results obtained with the B3LYP/6-311G(d,p) level of theory is the same, irrespective of the starting geometry. It has been observed that the structural parameters bond length, bond angles, and dihedral angles obtained from B3LYP/6-311G(d,p) and PBE1PBE/6-311G(d,p) level of theories are nearly the same as that of the values obtained at the MP2/6-311G(d,p) level of theory. The average root-mean-square deviation (rmsd) between the internal coordinates obtained from B3LYP and PBE1PBE methods is 0.028 and 0.039 Å for *cis*- and *trans*-isomers, respectively, and the average rmsd between the internal coordinates obtained from MP2 and B3LYP methods is 0.286 and 0.232 Å for *cis*- and *trans*-isomers, respectively. Hence, further discussions related with structure and vibrational frequency are based on the results obtained at the B3LYP/6-311G(d,p) level of theory. The optimized geometry of *cis*- and *trans*-isomers of the unsubstituted BNC molecule is shown in Figure 1. The selected structural parameters of unsubstituted BNC molecule are summarized in Table 2. It has been observed that the isomerization does not alter the bond length of unsubstituted BNC. The bond angles θ_2(C12−C14−C16), θ_4(C14−C12−H13), θ_5(C14−C16−O17), and θ_7(C16−C14−H15) and the dihedral angles Φ_6(O17−C16−C18-C19), Φ_7(O17−C16−C18−C23), and Φ_8(C19−C18−C16−C14) differ around 3−5 and 11−13° between *cis*- and *trans*-isomers of BNC (see Figure 1 and Table 2 for labeling of atoms and angles). The dihedral angles Φ_2-(C12−C14−C16−C18), Φ_4(O17−C16−C14−C12), and Φ_5-(O17−C16−C14−H15) corresponding to the *cis*- and *trans*-isomers, are 175, −5, and 172° and −22, 158, and −14°, respectively. It has been observed that the structural parameters are not significantly affected by the substitution of different EWG and EDG at the *para* and *meta* positions of BNC.

It has been observed that the structural parameters calculated at the cis/6-31+G(d,p) level of theory for *cis*- and *trans*-isomers in the excited state have the same trend as that of the ground state structure. It is noted that the bond length of the excited state structure has slightly decreased around 0.01 to 0.1 Å compared to the ground state structure. The bond angles differ by 2−4°, and the dihedral angles differ by 3−9° with respect to the ground

Table 2. Selected Geometrical Parameters (Bond Length in Å, Angle in Degrees) of Unsubstituted BNC at the B3LYP/6-311G(d,p) Level of Theory[a]

parameters	cis	trans
R_1(C3−C12)	1.461	1.464
R_2(C12−H13)	1.088	1.086
R_3(C12−C14)	1.345	1.346
R_4(C14−H15)	1.083	1.085
R_5(C16−C14)	1.487	1.480
R_6(C16−O17)	1.223	1.222
R_7(C16−C18)	1.505	1.506
R_8(C18−C19)	1.382	1.380
R_9(C19−C20)	1.406	1.408
R_{10}(C21−Br30)	1.922	1.923
θ_1(C12−C3−C2)	123.3	123.2
θ_2(C12−C14−C16)	120.2	125.8
θ_3(C14−C12−C3)	128.1	127.2
θ_4(C14−C12−H13)	115.9	118.0
θ_5(C14−C16−O17)	121.7	119.0
θ_6(C14−C16−C18)	117.3	119.9
θ_7(C16−C14−H15)	118.3	112.4
θ_8(C16−C18−C19)	118.4	118.8
θ_9(O17−C16−C18)	121.7	121.1
θ_{10}(Br30−C21−C20)	117.3	117.4
Φ_1(C3−C12−C14−C16)	178.5	−174.6
Φ_2(C12−C14−C16−C18)	174.8	−21.5
Φ_3(C16−C18−C19−C20)	−176.3	−175.8
Φ_4(O17−C16−C14−C12)	−5.4	158.5
Φ_5(O17−C16−C14−H15)	172.3	−14.4
Φ_6(O17−C16−C18−C19)	145.5	132.8
Φ_7(O17−C16−C18−C23)	−31.5	−43.0
Φ_8(C19−C18−C16−C14)	−34.6	−47.3
Φ_9(Br30−C21−C22−C24)	0.892	0.718

[a] For labeling of atoms, see Figure 1.

Table 3. Selected Scaled Vibrational Frequencies (cm^{-1}) and Assignment for Unsubstituted *Cis*- and *Trans*-Isomers of BNC Calculated at the B3LYP/6-311G(d,p) Level of Theory

Vibrational Frequencies (cm^{-1})		Assignment
Cis	Trans	
3083	3083	SP^2 C-H stretching
1668	1649	C=O stretching
1584	1550	C=C stretching of α-β aliphatic unsaturated carbon
1491	1491	C=C stretching in aromatic ring
1308	-	C-CO-C skeletal stretching
1204,1077	1229,1222	Inplane C-H bending of aromatic ring
-	867	scissoring mode of vibration of symmetric >−< stretching
955	967	scissoring mode of vibration of asymmetric >−< stretching
756	757	C-H bending of hydrogen attached to α-β unsaturated carbon
706	680	C-H bending in benzene ring

Table 4. Ground State Molecular Orbital Energies (E_{HOMO}, E_{LUMO}) and Energy Gap (ΔE; in eV) of Unsubstituted and Substituted *Trans*-BNC Calculated at the PBE1PBE/6-311G(d,p) Level of Theory in Ethanol Medium

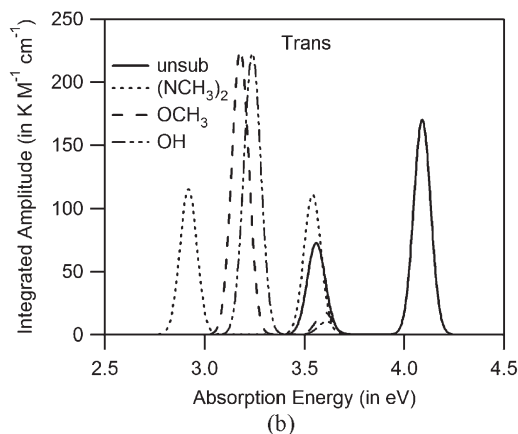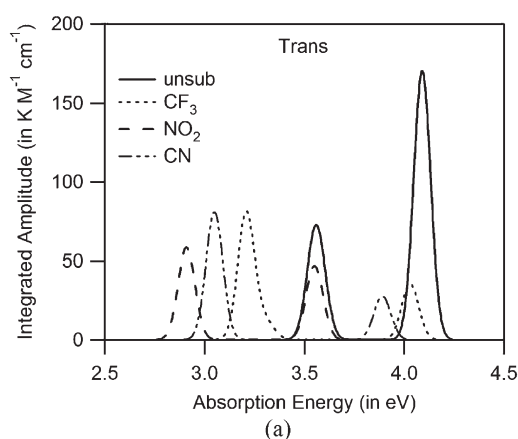| BNC molecule	E_{HOMO}	E_{LUMO}	ΔE
unsubstituted	−6.53	−2.45	4.08
CF$_3$	−6.80	−2.72	4.08
NO$_2$	−6.80	−3.27	3.53
CN	−6.80	−2.99	3.81
N(CH$_3$)$_2$	−5.71	−2.18	3.53
OCH$_3$	−6.26	−2.45	3.81
OH	−6.26	−2.45	3.81

Table 5. Computed Absorption Energies (in eV and in nm) and Oscillator Strengths (in a.u.) of Unsubstituted, EWG- and EDG-Substituted Trans-BNC at the PBE1PBE/6-311G(D,P) Level of Theory in Ethanol Medium

		absorption energies[a]		oscillator
BNC molecule	orbital transitions[b]	eV	nm	strength f (a.u.)
unsubstituted	H→L (0.562)	3.55	350	0.20
	H −2→L (0.438)	3.58	347	0.084
	H-1→L (0.631)	4.09	303	0.631
CF$_3$	H→L (0.663)	3.21	386	0.299
	H-3→L (0.536)	3.31	374	0.041
	H-2→L (0.585)	4.03	307	0.132
NO$_2$	H→L (0.688)	2.91	425	0.217
	H→L+1 (0.670)	3.55	349	0.174
CN	H→L (0.691)	3.05	407	0.30
	H-2→L (0.616)	3.89	319	0.103
N(CH$_3$)$_2$	H→L (0.696)	2.92	424	0.428
	H-1→L (0.513)	3.54	351	0.413
OCH$_3$	H→L (0.685)	3.18	390	0.837
	H-1→L (0.673)	3.60	344	0.066
OH	H→L (0.675)	3.24	383	0.826
	H-1→L (0.666)	3.61	343	0.038

[a] Only the transitions with an oscillator strength higher than 0.01 a.u. are given. [b] H and L indicate HOMO and LUMO, respectively. Value given within parentheses is the orbital coefficient.

Figure 2. The absorption spectra of unsubstituted and (a) electron withdrawing groups (b) electron donating groups substituted BNC computed at PBE1PBE/6-311G(d,p) level of theory in ethanol medium. (The spectra were simulated by using a Gaussian distribution centered at the computed absorption energies with an arbitrary width of 0.05 eV and an integrated amplitude equal to the calculated oscillator strengths).

state structure. The calculated total energy for excited state geometry in ethanol medium shows that for unsubstituted and NO$_2$-, CN-, N(CH$_3$)$_2$-substituted BNC, the *cis*-structure is relatively stable, but the relative energy is around 0.5 kcal/mol only, whereas for CF$_3$-, OCH$_3$-, and OH-substituted BNC, the *trans*-structure is relatively stable by 1 kcal/mol. Hence, in the present study, the absorption and emission spectra were calculated and discussed only for the *trans*-isomer of BNC.

The dipole moment of the unsubstituted and substituted *trans*-BNC molecules in gas and solvent phases calculated at the B3LYP/6-311G(d,p) level of theory are summarized in Table 1. The dipole moment of unsubstituted BNC is 3.60 D in the gas phase. The substitution of EWG and EDG on BNC alters the delocalization of electron density and influences the dipole moment. The substitution of EWG and EDG enhances the dipole moment of the BNC molecule except for the CF$_3$-substituted

BNC for which the dipole moment is 2.52 D. The dipole moment of unsubstituted and substituted BNC molecules in ethanol medium has increased, except for the CF$_3$-substituted BNC molecule. Among the substituted BNC molecules, the N-(CH$_3$)$_2$-substituted chalcone has a maximum dipole moment value of 6.23 and 8.96 D in gas and ethanol medium, respectively.

3.2. Vibrational Frequency Analysis. The calculated harmonic vibrational frequencies at the B3LYP/6-311G(d,p) level of theory indicate that the optimized structure of unsubstituted and substituted BNC molecules are at stationary point without any imaginary frequency. The calculated frequencies were scaled with the standard value of 0.9679 for the B3LYP/6-311G(d,p) level of theory.[42] The selected vibrational frequencies of the two isomers of unsubstituted BNC have been assigned[43−45] and are given in Table 3. Both *cis*- and *trans*-isomers have a similar mode of vibrations, except the scissoring mode of vibration of the aliphatic ⟩C=C⟨ group. In the *cis*-isomer, the alkene carbon has *trans*-hydrogen atoms, and the change in dipole moment is zero for symmetric stretching. Hence, the vibration mode around 867 cm^{-1} that appeared in the *trans*-isomer was absent in the *cis*-isomer. However, the mode corresponding to the asymmetric stretching vibration has appeared around 955 and 967 cm^{-1}
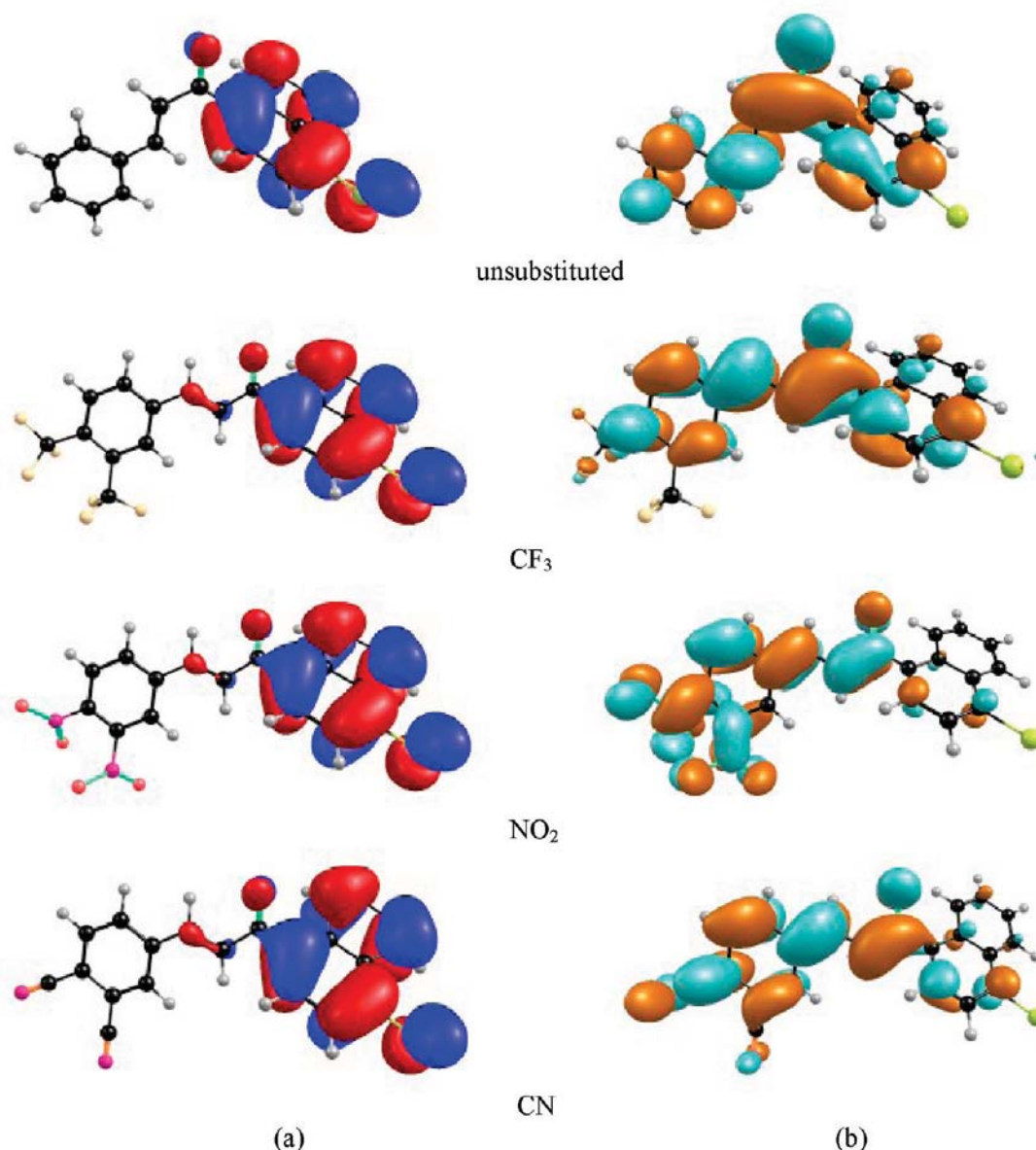
Figure 3. Density plot of the (a) HOMO and (b) LUMO of the unsubstituted and CF₃-, NO₂-, and CN-substituted *trans*-BNC calculated at the PBE1PBE/6-311G(d,p) level of theory in ethanol medium.

for *cis*- and *trans*-isomers, respectively. The vibrational mode corresponding to carbonyl stretching in the *cis*- and *trans*-isomers is 1668 and 1649 cm^{-1}, which is in agreement with the previous experimental values of 1687 and 1657 cm^{-1}.[13] The substitution of the EWG and EDG at para and meta positions does not alter the vibrational modes of BNC, and the maximum difference of 20 cm^{-1} is noted with respect to the unsubstituted BNC. The carbonyl stretching frequency in the *cis*-isomer is higher than that of the *trans*-isomer. This is due to relatively greater strain interaction between the bulky naphthalene group and the C═O group in the *cis*-isomers.[13] However, in the present study, the *cis*- and *trans*-isomers of substituted BNC molecules have a similar C═O stretching frequency. This is due to change in steric interaction between the groups upon the substitution of EWG and EDG on BNC.

3.3. Absorption Spectra of Unsubstituted and Substituted BNC. The spectral studies of unsubstituted, EWG- and

EDG-substituted BNC have been performed for the *trans*-isomer using a time-dependent DFT calculation at B3LYP/6-311G(d,p) and PBE1PBE/6-311G(d,p) levels of theory in gas and solvent phases. The calculated absorption energy, corresponding oscillator strength, and orbital coefficients are summarized in Tables 5 and S1. To obtain the nature and the energy of the singlet–singlet electronic transition, the first three low lying excited states have been calculated. The absorption energies with oscillator strength greater than 0.01 are considered throughout the discussion. Previous spectral studies on chalcones reveal that the spectral properties calculated at PBE1PBE method in ethanol medium agree well with the experimental value.[29] While comparing PBE1PBE and B3LYP results in gas and solvent phases, it has been observed that the absorption spectra of BNC have slightly shifted to a higher wavelength region in the B3LYP method. A maximum shift of 36 nm is observed for NO₂-substituted BNC,
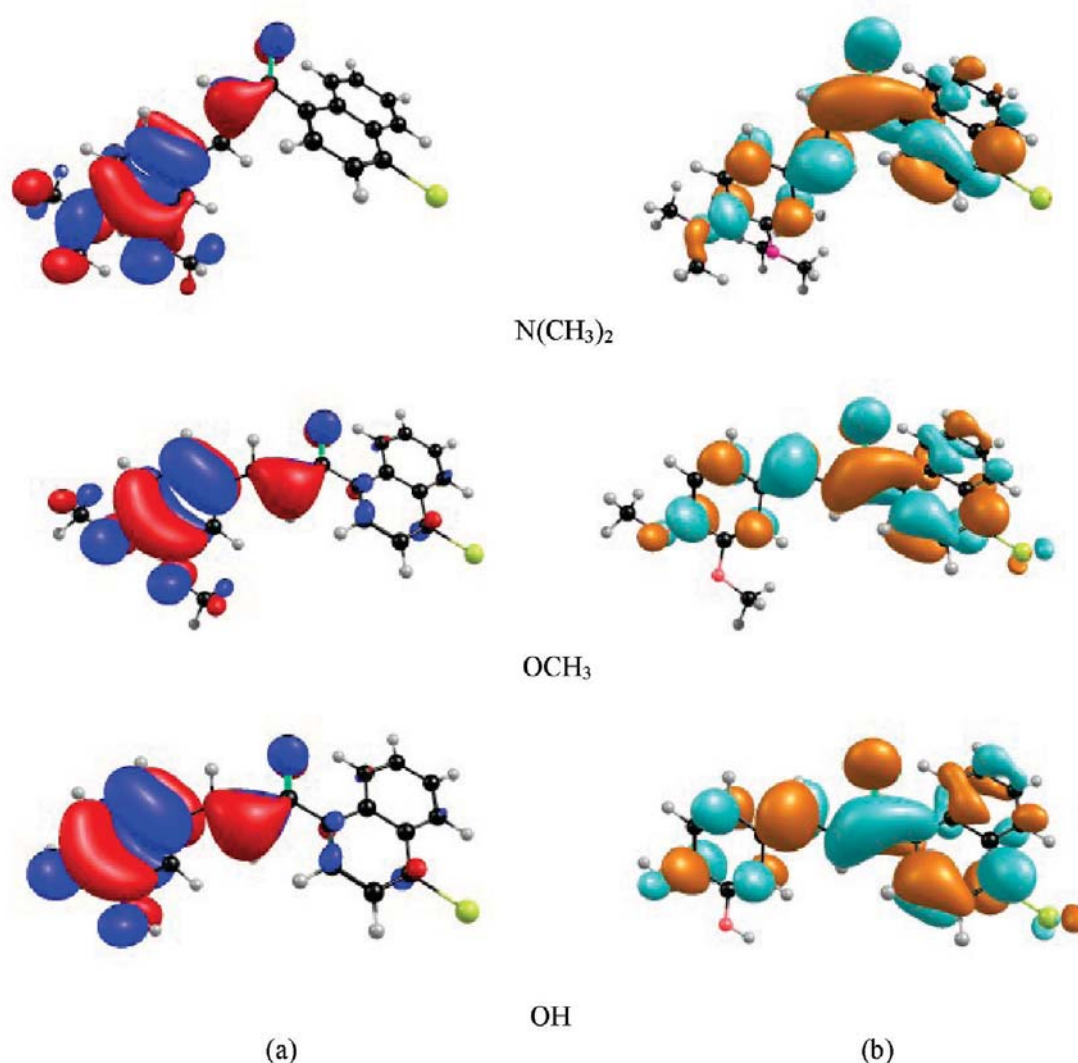
Figure 4. Density plot of the (a) HOMO and (b) LUMO of the $N(CH_3)_2$-, OCH_3-, and OH-substituted *trans*-BNC calculated at the PBE1PBE/6-311G(d,p) level of theory in ethanol medium.

and for other BNC molecules, the shift is within 25 nm. Except for a few cases, the orbital transitions corresponding to dominant absorption bands are similar in PBE1PBE and B3LYP methods. Here, the absorption spectra calculated at PBE1PBE/6-311G(d,p) level of theory in ethanol medium has been discussed in detail.

The TDDFT results given in Table 5 show that for both unsubstituted and substituted BNC, the lowest energy transition is due to the excitation of electron from highest occupied molecular orbital (HOMO) to the lowest unoccupied molecular orbital (LUMO). The absorption intensity is directly related with the dimensionless oscillator strength value and the dominant absorption bands are the transitions with higher oscillator strength value. The absorption energies calculated at PBE1PBE/6-311G(d,p) level of theory in ethanol medium were plotted with respect to integrated amplitude derived from oscillator strength and is shown in Figure 2. The absorption spectra of unsubstitued BNC has two features and the dominant absorption band is observed at 4.09 eV (303 nm) which is associated with HOMO-1→LUMO transition. The second intense band is observed around 3.56 eV (348 nm) which corresponds to HOMO→LUMO and HOMO-2→LUMO transitions. The absorption spectra of EWG-substituted BNC molecules

possess one intense peak and one less intense peak except for NO_2-substituted BNC in which both the peaks are intense. The dominant absorption band has been observed at 3.21 eV (386 nm), 2.91 eV (425 nm) and 3.05 eV (407 nm) for CF_3-, NO_2- and CN-substituted BNC molecules, respectively. From Figure 2b it has been observed that $N(CH_3)_2$-substituted BNC has two sharp features, whereas the OCH_3- and OH-substituted BNC have one intense feature. The dominant absorption band for $N(CH_3)_2$-, OCH_3- and OH-substituted BNC has been noted at 2.92 eV (424 nm), 3.18 eV (390 nm) and 3.24 eV (383 nm) corresponding to the excitation of electron from HOMO→LUMO. The $N(CH_3)_2$-substituted BNC has the second intense absorption band at 3.54 eV (351 nm), which corresponds to HOMO-1→LUMO transition. It has been observed from Figure 2 that the dominant absorption band of the unsubstituted BNC lies at the lower wavelength region whereas the dominant absorption bands of EWG- and EDG-substituted BNC lies at the higher wavelength region of the spectrum.

In agreement with the earlier spectral studies on chalcones,[29] the absorption spectrum corresponding to the first excited state (HOMO → LUMO) calculated at B3LYP/6-311G(d,p) and PBE1PBE/6-311G(d,p) levels of theory exhibits bathochromic

Table 6. Computed Emission Energies (in eV and in nm) and Oscillator Strengths (in a.u.) of Unsubstituted, EWG- and EDG-Substituted *Trans*-BNC at the PBE1PBE/6-311G(d,p) Level of Theory in Ethanol Medium

| BNC molecule | orbital transitions[b] | emission energies[a] | | oscillator strength f (a.u.) |
		eV	nm	
unsubstituted	H-1→L (0.588)	3.58	346	0.963
CF_3	H→L (0.695)	2.80	442	0.192
	H-1→L (0.699)	3.47	357	0.971
NO_2	H→L (0.703)	2.40	518	0.145
	H-1→L (0.678)	3.20	387	0.983
CN	H→L (0.702)	2.60	476	0.155
	H-1→L (0.694)	3.36	369	1.149
$N(CH_3)_2$	H→L (0.684)	2.79	444	0.757
	H-2→L (0.448)	3.39	366	0.115
	H-3→L (0.447)			
OCH_3	H→L (0.683)	3.03	409	1.105
	H-1→L (0.659)	3.45	360	0.014
OH	H→L (0.660)	3.09	401	1.024
	H-2→L (0.619)	3.19	388	0.037
	H-1→L (0.657)	3.42	362	0.030

[a] Only the transitions with oscillator strength higher than 0.01 a.u. are given. [b] H and L indicate HOMO and LUMO, respectively. Value given within the parentheses is the orbital coefficient.

Figure 5. Optical emission spectra of unsubstituted, (a) electron with-drawing groups and (b) electron donating groups substituted BNC computed at the PBE1PBE/6-311G(d,p) level of theory in ethanol medium. (The spectra were simulated by using a Gaussian distribution centered at the computed absorption energies with an arbitrary width of 0.05 eV and an integrated amplitude equal to the calculated oscillator strengths.)

effects when different EWGs and EDGs are substituted at the para and meta positions of the BNC in both gas and solvent phases. It has been observed that the EWG-substituted BNC exhibits larger bathochromic displacement than the EDG-substituted BNC. In the gas phase, the largest displacement of +78 nm is observed for the NO_2-substituted BNC and the smallest displacement of +25 nm is observed for OH-substituted BNC at the PBE1PBE/6-311G(d,p) level of theory. In the solvent phase, the NO_2-substituted BNC exhibits the largest displacement of +75 nm and OH-substituted BNC possesses the smallest displacement of +33 nm at the PBE1PBE/6-311G(d,p) level of theory. In agreement with previous studies,[27,29] the substitutions affect the oscillator strength values. The substitution of OCH_3 and OH groups increases the oscillator strength value compared to other substitutions both in gas and solvent phases. From Table 5 and S1c it has been observed that the polar environment influences the absorption spectrum and oscillator strength of BNC molecules. The absorption spectrum of un-substituted and EDG-substituted BNC in ethanol medium shifts toward a higher wavelength region in both B3LYP and PBE1PBE methods. A maximum shift of about 40 nm is observed for $N(CH_3)_2$-substituted BNC, whereas in EWG-substituted BNC, the spectrum shifts slightly to a lower wavelength region and the shift is within 15 nm.

3.4. Molecular Orbitals of Unsubstituted and Substituted BNC. The density plot of the HOMO, LUMO, and HOMO-1 of unsubstituted and substituted BNC molecules calculated at the PBE1PBE/6-311G(d,p) level of theory in ethanol medium is shown in Figures 3, 4, and S1, respectively. The orbital diagrams were plotted with the contour value of 0.025 a.u. As shown in Figure 3, the HOMO of unsubstituted BNC is delocalized mainly on the naphthyl group and the LUMO is delocalized over the
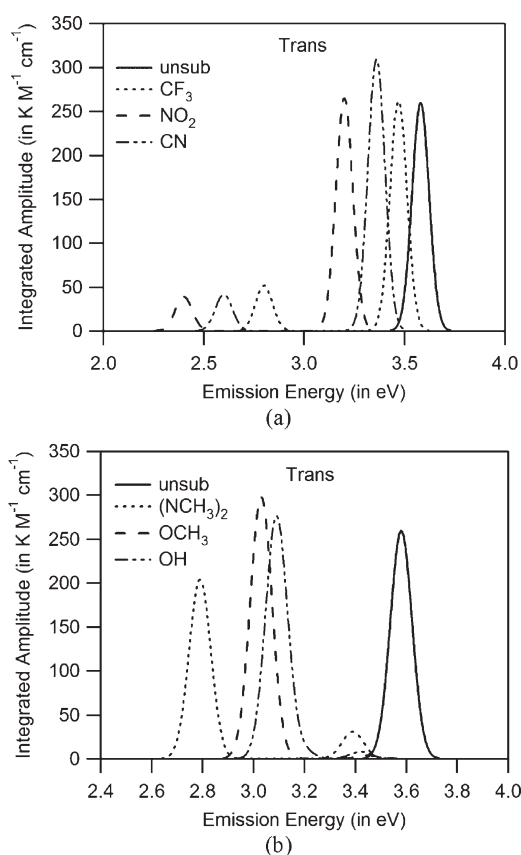
entire molecule. The HOMO of the CF_3-, NO_2-, and CN-substituted BNC molecule is localized on the main chain as well as on the naphthyl group, whereas the LUMO extends over the entire molecule. The HOMO of $N(CH_3)_2$-substituted BNC molecule is localized on the phenyl ring and on the main chain. The HOMO and LUMO of OCH_3- and OH-substituted BNC molecules are dis-tributed over the entire molecule. It has been observed that the HOMO-1 of unsubstituted and $N(CH_3)_2$-substituted BNC is localized on the phenyl ring and on the main chain, whereas the HOMO-1 of CF_3-, NO_2-, CN-, OCH_3-, and OH-substituted BNC is delocalized over the entire molecule. The above results show that the substitution of EWG and EDG significantly alters the spatial charge distribution on the BNC molecule and alters the spectral properties. The energies of HOMO, LUMO, and the energy gap between them for the ground state *trans*-BNC isomer calculated at the PBE1PBE/6-311G(d,p) level of theory in the solvent phase have been summarized in Table 4. It has been observed that the absorption energy calculated at the TD-PBE1PBE/6-311G(d,p) level of theory corresponding to the HOMO → LUMO transition is comparable with the energy gap value. The calculated HOMO−LUMO (H-L) energy gap of unsubstituted BNC is found to be 4.08 eV. It has been observed that the H-L energy gap slightly decreases upon the substitution of EWG and EDG in the BNC molecule. The NO_2- and $N(CH_3)_2$-substituted BNC have a minimum H-L energy gap of

3.53 eV. It has been observed that the calculated (HOMO-1)−LUMO energy gap of the BNC molecule is found to be comparable with the HOMO−LUMO energy gap values. The (HOMO-1)−LUMO energy gap of unsubstituted BNC is 4.63 eV. The $N(CH_3)_2$-, OCH_3-, and OH-substituted BNC have a minimum (HOMO-1)−LUMO energy gap of 4.08 eV. As expected, the structures with small H-L energy gaps possess a minimum absorption energy or maximum absorption wavelength.

3.5. Emission Spectra of Unsubstituted and Substituted BNC. The excited state geometry of unsubstituted and substituted BNC molecules has been optimized by using the singly excited configuration interaction (CIS) method with the 6-31+G(d,p) basis set in the gas and solvent phases. The emission energies were computed for the first three excited states using TD-B3LYP/6-311G(d,p) and TD-PBE1PBE/6-311G(d,p) levels of theory in gas and solvent phases. The calculated emission energy, corresponding oscillator strength and orbital coefficients are summarized in Tables 6 and S2. Similar to absorption spectra, the emission spectra calculated at the TD-B3LYP method in gas and ethanol medium have shifted slightly to a higher wavelength while comparing with TD-PBE1PBE results. For NO_2-substituted BNC, a maximum shift of 48 nm is observed in ethanol medium. Except for a few cases, the orbital transitions corresponding to dominant emission bands are similar in PBE1PBE and B3LYP methods. The emission spectra calculated at the PBE1PBE/6-311G(d,p) level of theory in ethanol medium has been discussed in detail. It has been observed that for both unsubstituted and substituted BNC, the first excited state is due to the electronic transition between HOMO and LUMO, which is a very weak transition in unsubstituted BNC. The first excited state with a maximum emission wavelength is noted at 518 nm for the NO_2-substituted BNC.

The emission energies of unsubstituted, EWG- and EDG-substituted BNC calculated at the PBE1PBE/6-311G(d,p) level of theory in ethanol medium were plotted with respect to the integrated amplitude and are shown in Figure 5. From Figure 5a, it has been observed that the dominant emission band for unsubstituted BNC is noted at 3.58 eV (346 nm), which is associated with the HOMO-1 → LUMO transition. For CF_3-, NO_2-, and CN-substituted BNC, the dominant emission band is observed at 3.47 eV (357 nm), 3.20 eV (387 nm), and 3.36 eV (369 nm), respectively. The dominant emission band observed in CF_3-, NO_2-, and CN-substituted BNC is due to the electronic transition between HOMO-1 and LUMO. The $N(CH_3)_2$-, OCH_3-, and OH-substituted BNC possess the dominant emission band at 2.79 eV (444 nm), 3.03 eV (409 nm), and 3.09 eV (401 nm), and these emission bands are associated with the HOMO → LUMO transition. The above results show that the substitution of EWG and EDG on BNC increases the emission wavelength. The polar environment influences the emission spectrum and oscillator strength of BNC molecules. The emission spectrum of unsubstituted and EWG-substituted BNC in ethanol medium shifts slightly to a lower wavelength region, and for EDG-substituted BNC, the spectrum shifts slightly to a higher wavelength region.

4. CONCLUSIONS

The DFT and CIS calculations were used to investigate the spectral properties of unsubstituted and different electron withdrawing and donating groups substituted 4-bromo-1-naphthyl chalcones (BNC) in gas and solvent phases. The calculated relative energy of unsubstituted and substituted BNC molecules show that the *trans*-isomer is more stable than the *cis*-isomer with a very small

energy difference. The substitution of different EWG and EDG at para and meta positions of BNC enhances the stability of the *trans*-isomer. It has been observed that the dipole moment of ground state BNC has significantly changed with the substitutions, and the dipole moment of BNC increases in ethanol medium. The calculated vibrational frequencies of the two isomers were assigned for the respective vibrations and compared with an available experimental value. The absorption and emission spectra have been calculated using the TDDFT method at the B3LYP/6-311G(d,p) and PBE1PBE/6-311G(d,p) levels of theory in gas and ethanol medium. It has been observed that the spectra have shifted slightly toward higher wavelength region in B3LYP method compared to PBE1PBE method. A maximum difference of around 40 nm is observed for NO_2-substituted BNC both in absorption and in emission spectra. The substitution of different electron donating and withdrawing groups significantly alters the absorption and emission properties of BNC. The absorption and emission spectra of BNC shifted to a lower wavelength region upon the substitution of EWG and the substitution of EDG shifts the spectra to a higher wavelength region. In ethanol medium for unsubstituted BNC, the dominant emission band is observed at 346 nm, and for NO_2- and $N(CH_3)_2$-substituted BNC, the dominant bands are observed at 387 and 444 nm, respectively. The results obtained from this investigation confirm that the spectral properties of BNC molecules can be tuned by the suitable substitution and are used to design novel and efficient LEDs.

■ ASSOCIATED CONTENT

Ⓢ **Supporting Information.** The absorption and emission spectra calculated at B3LYP/6-311G(d,p) and PBE1PBE/6-311G(d,p) levels of theory for unsubstituted and different EWG- and EDG-substituted *trans*-BNC in gas and ethanol medium are summarized in Tables S1 and S2. The density plot of the HOMO-1 of unsubstituted and substituted *trans*-BNC calculated at the PBE1PBE/6-311G(d,p) level of theory in ethanol medium is shown in Figure S1. This material is available free of charge via the Internet at http://pubs.acs.org.

■ AUTHOR INFORMATION

Corresponding Author
*Fax: +91-422-2422387. E-mail: ksenthil@buc.edu.in.

■ ACKNOWLEDGMENT

■ REFERENCES

(1) Cockerman, M. P.; Frazier, C. C.; Guha, S.; Chauchard, E. A. *Appl. Phys. B: Laser Opt.* **1991**, *53*, 275.

(2) Zaho, B.; Zhang, D.; Cao, Y.; Chen, W. J.; Sun, Z. R.; Wang, Z. G. *Acta Phys. Chim. Sin.* **2000**, *16*, 422.

(3) Mager, L.; Melzer, C.; Barzoukas, M.; Fort, A.; Mery, S.; Nicoud, J. F. *Appl. Phys. Lett.* **1997**, *71*, 2248.

(4) Monroe, B.; Smothers, W. K.; Keys, E. D.; Krebs, R. R.; Mickish, J. D.; Harrington, F. A.; Schicker, S. R.; Armstrong, K. M.; Chan, D. M. T.; Weathers, I. C. *J. Imaging Sci.* **1991**, *35*, 19.

(5) Anto, R. J.; Sukumarana, K.; Kuttana, G.; Raob, M. N.; Subbarajuc, V.; Kuttana, R. *Cancer Lett.* **1995**, *97*, 33.

(6) Liu, M.; Wilairat, P.; Go, M. L. *J. Med. Chem.* **2001**, *44*, 4443.

6601

dx.doi.org/10.1021/jp1098393 |*J. Phys. Chem. A* 2011, 115, 6594–6602

(7) Murakami, S.; Muramatsu, M.; Aihara, H. *Biochem. Pharmacol.* **1991**, *42*, 1447.

(8) Dhar, D. N. *The Chemistry of Chalcones and Related Compounds*; Wiley-Interscience: New York, 1981.

(9) Batovska, D.; Parushev, S.; Slavova, A.; Bankova, V.; Tsvetkova, I.; Ninova, M.; Najdenski, H. *Eur. J. Med. Chem.* **2007**, *42*, 87.

(10) Rurack, K.; Bricks, J. L.; Reck, G.; Radeglia, R.; Resch-Genger, U. *J. Phys. Chem. A* **2000**, *104*, 3087.

(11) Rurack, K.; Dekhtyar, M. L.; Bricks, J. L.; Resch-Genger, U. *J. Phys. Chem. A* **1999**, *103*, 9626.

(12) Wang, P.; Wu, S. *J. Photochem. Photobiol., A* **1995**, *86*, 109.

(13) Thirunarayanan, G.; Gopalakrishnan, M.; Vanagamudi, G. *Spectrachim. Acta, Part A* **2007**, *67*, 1106.

(14) Casida, M. E. In *Recent Advances in Density Functional Methods, Part I*; Chong, D. P., Ed.; World Scientific: Singapore, 1995.

(15) Gross, E. K. U.; Dobson, J. F.; Petersilka, M. In *Density Functional Theory II*; Nalewajski, R. F., Ed.; Springer: Heidelberg. 1996.

(16) Foresman, J. B.; Head-Gordon, M.; Pople, J. A; Frisch, M. J. *J. Phys. Chem.* **1992**, *96*, 135.

(17) Petit, L.; Adamo, C.; Russo, N. *J. Phys. Chem. B* **2005**, *109*, 12214.

(18) Jacquemin, D.; Preat, J.; Wathelet, V.; Fontaine, M.; Perpete, E. A. *J. Am. Chem. Soc.* **2006**, *128*, 2072.

(19) Pezzella, A.; Panzella, L.; Crescenzi, O.; Napolitano, A.; Navaratman, S.; Edge, R.; Land, E. J.; Barone, V.; d'Ischia, M. *J. Am. Chem. Soc.* **2006**, *128*, 15490.

(20) Improta, R.; Barone, V.; Santoro, F. *Angew. Chem., Int. Ed.* **2007**, *46*, 405.

(21) Ciofini, I.; Adamo, C. *J. Phys. Chem. A* **2007**, *111*, 5549.

(22) Burke, K.; Werschnik, J.; Gross, E. K. U. *J. Chem. Phys.* **2005**, *123*, 062206.

(23) Li, X.; Liu, X.; Wu, Z.; Zhang, H. *J. Phys. Chem. A* **2008**, *112*, 11190.

(24) Li, W.; Wang, Y.-B.; Pavel, I.; Yuan, Q.; Ye, Y.; Fu, E.-Q.; Luo, M.-D.; Hu, J.-M.; Kiefer, W. *J. Phys. Chem. A* **2005**, *109*, 2878.

(25) Dreuw, A.; Head-Gordon, M. *J. Am. Chem. Soc.* **2004**, *126*, 4007.

(26) Dreuw, A.; Weisman, J. L.; Head-Gordon, M. *J. Chem. Phys.* **2003**, *119*, 2943.

(27) Santhanamoorthi, N.; Senthilkumar, K.; Kolandaivel, P. *Mol. Phys.* **2009**, *107*, 1629.

(28) Wang, J.; Gu, J.; Leszczynski, J. *Chem. Phys. Lett.* **2008**, *456*, 206.

(29) Xue, Y.; Mou, J.; Liu, Y.; Gong, X.; Yang, Y.; An, L. *Cent. Eur. J. Chem.* **2010**, *8*, 928.

(30) Becke, A. D. *J. Chem. Phys.* **1993**, *98*, 5648.

(31) Lee, C. T.; Yang, W. T.; Parr, R. G. *Phys. Rev. B* **1988**, *37*, 785.

(32) Vosko, S. H.; Wilk, L.; Nusair, M. *Can. J. Phys.* **1980**, *58*, 1200.

(33) Stephens, P. J.; Devlin, F. J.; Chabalowski, C. F.; Frisch, M. J. *J. Phys. Chem. Lett.* **1994**, *98*, 11623.

(34) Perdew, J. P.; Burke, K.; Ernzerhof, M. *Phys. Rev. Lett.* **1996**, *77*, 3865.

(35) Perdew, J. P.; Burke, K.; Ernzerhof, M. *Phys. Rev. Lett.* **1997**, *78*, 1396.

(36) Adamo, C.; Barone, V. *J. Chem. Phys.* **1999**, *110*, 6158.

(37) Ernzerhof, M.; Scuseria, G. E. *J. Chem. Phys.* **1999**, *110*, 5029.

(38) Moller, C.; Plesset, M. S. *Phys. Rev.* **1934**, *46*, 618.

(39) Miertus, S.; Scrocco, E.; Tomasi, J. *Chem. Phys.* **1981**, *55*, 117.

(40) Frisch, M. J.; Trucos, G. W.; Schlegel, H. B.; Scuseria, G. E.; Robb, M. A.; Cheeseman, J. R.; Scalmani, G.; Barone, V.; Mennucci, B.; Petersson, G. A.; Nakatsuji, H.; Caricato, M.; Li, X.; Hratchian, H. P.; Izmaylov, A. F.; Bloino, J.; Zheng, G.; Sonnenberg, J. L.; Hada, M.; Ehara, M.; Toyota, K.; Fukuda, R.; Hasegawa, J.; Ishida, M.; Nakajima, T.; Honda, Y.; Kitao, O.; Nakai, H.; Vreven, T.; Montgomery, J. A., Jr.; Peralta, J. E.; Ogliaro, F.; Bearpark, M.; Hevd, J. J.; Brothers, E.; Kudin, K. N.; Staroverov, V. N.; Kobayashi, R.; Normand, J.; Raghavachari, K.; Rendell, A.; Burant, J. C.; Iyengar, S. S.; Tomasi, J.; Cossi, M.; Rega, N.; Millam, J. M.; Klene, M.; Knox, J. E.; Cross, J. B.; Bakken, V.; Adamo, C.; Jaramillo, J.; Gomperts, R.; Stratmann, R. E.; Yazyev, O.; Austin, A. J.; Cammi, R.; Pomelli, C.; Ochterski, J. W.; Martin, R. L.; Morokuma, K.; Zakrzewski, V. G.; Voth, G. A.; Salvador, P.; Dannenberg, J. J.; Dapprich, S.; Daniels, A. D.; Farkas, O.; Foresman, J. B.; Ortiz, J. V.; Cioslowski, J.; and Fox, D. J. *Gaussian 09*, Revision A.02; Gaussian, Inc.: Wallingford, CT, 2009.

(41) Xue, Y.; Gong, X. *J. Mol. Struct. (THEOCHEM)* **2009**, *901*, 226.

(42) Andersson, M. P.; Uvdal, P. *J. Phys. Chem. A* **2005**, *109*, 2937.

(43) Sharma, Y. R. *Elementary Organic Spectroscopy Principles and Chemical Applications*, 3rd ed.; S. Chand and Company, Ltd.: New Delhi, India, 1999.

(44) Pavia, D. L.; Lampman, G. M.; Kriz, G. S. *Introduction to Spectroscopy*, 3rd ed.; Harcourt College Publishers: India, 2001.

(45) Silverstein, R. M.; Webster, F. X. *Spectrometric Indentification of Organic Compounds*, 6th ed.; John Wiley and Sons, Inc.: New York, 2002.